



Generalized maximum likelihood estimators for the nonstationary generalized extreme value model

S. El Adlouni,¹ T. B. M. J. Ouarda,¹ X. Zhang,² R. Roy,³ and B. Bobée¹

Received 31 August 2005; revised 21 March 2006; accepted 26 September 2006; published 8 March 2007.

[1] The objective of the present study is to develop efficient estimation methods for the use of the GEV distribution for quantile estimation in the presence of nonstationarity. Parameter estimation in the nonstationary GEV model is generally done with the maximum likelihood estimation method (ML). In this work, we develop the generalized maximum likelihood estimation method (GML), in which covariates are incorporated into parameters. A simulation study is carried out to compare the performances of the GML and the ML methods in the case of the stationary GEV model (GEV0), the nonstationary case with a linear dependence of the location parameter on covariates (GEV1), the nonstationary case with a quadratic dependence on covariates (GEV2), and the nonstationary case with linear dependence in both location and scale parameters (GEV11). Simulation results show that the GML method performs better than the ML method for all studied cases. The nonstationary GEV model is also applied to a case study to illustrate its potential. The case study deals with the annual maximum precipitation at the Randsburg station in California, and the covariate process is taken to be the Southern Index Oscillation.

Citation: El Adlouni, S., T. B. M. J. Ouarda, X. Zhang, R. Roy, and B. Bobée (2007), Generalized maximum likelihood estimators for the nonstationary generalized extreme value model, *Water Resour. Res.*, 43, W03410, doi:10.1029/2005WR004545.

1. Introduction

[2] Extreme value analysis of hydrometeorological data allows interpreting past records and making inference about future probabilities of occurrence of extreme events, such as floods, extreme rainfalls, or wind speeds. Extreme values are often represented by the maximum value of a given variable over a time period such as a year. Extreme value theory indicates that these maxima can generally be described by one of the three extreme value distributions that can be generalized as the generalized extreme value (GEV) distribution [e.g., *Jenkinson*, 1955]. This GEV distribution has three parameters. It is among the most frequently used distributions for extreme value analysis [*Stedinger et al.*, 1993; *Ouarda et al.*, 2001; *Katz et al.*, 2002] in hydrology and climatology. Several methods have been developed for the estimation of GEV distribution parameters. They include the method of maximum likelihood (ML) [*Smith*, 1985], the method of moments (MM) [*Madsen et al.*, 1997], the method of L moments (LM) [*Hosking*, 1990], and the method of probability weighted moments (PWM) [*Hosking et al.*, 1985]. A comprehensive

review of recent developments in extreme value analysis in hydrology is presented by *Katz et al.* [2002].

[3] There are two fundamental assumptions for the classical frequency analysis to provide useful engineering design values. The proper estimation of design values requires that the data series from which the probability distribution parameters are to be estimated come from independent and identically distributed (iid) observations. The proper assessment of risk factors for an engineering structure requires that the statistical inference has also to be valid during the projected life span of the structure. This requires that the conditions (e.g., climate) under which the inferences are made will remain the same in the future. There are, however, mounting evidence suggesting that such assumptions can hardly be met in reality. On the one hand, observed historical extreme events are hardly nonstationary. In fact, statistically significant trends have been identified in extreme values of different hydroclimatological series [*Intergovernmental Panel on Climate Change*, 2001] in different parts of the world. On the other hand, the anthropogenic influence on the climate system caused by the increase in the emission of greenhouse gases into the atmosphere has a potential to make future climate very different from what it is today. Climate extremes will likely change in the future [e.g., *Jain and Lall*, 2001; *Wang et al.*, 2004; *Wang and Swail*, 2004; *Kharin and Zwiers*, 2005]. The reality of nonstationary hydrometeorological extremes needs to be properly addressed since the GEV model with constant parameters may no longer be valid under nonstationary conditions [*Leadbetter et al.*, 1983].

[4] Nonstationarity of extreme values may be detected by identifying trends in the extreme values [e.g., *Zhang et al.*,

¹Centre Eau, Terre and Environnement, Institut National de la Recherche Scientifique, University of Quebec, Quebec, Quebec, Canada.

²Climate Research Branch, Climate Monitoring and Data Interpretation Division, Meteorological Service of Canada, Environment Canada, Downsview, Ontario, Canada.

³OURANOS Consortium on Climate Change, Montreal, Quebec, Canada.

2001, 2004; Clarke, 2002]. In this situation, “covariates” may be introduced into the probability distribution when modeling extreme values [Smith, 1989] in order to determine conditional distributions. Scarf [1992] introduced a trend in the position parameter for the GEV model. Coles [2001] provided a general description of the covariate approach to the modeling of extreme values. An example of hydrological application of the covariate approach is given by Katz *et al.* [2002]. Sankarasubramanian and Lall [2003] studied quantile regression with climate indicators to estimate quantiles under climate change conditions. The covariate approach has also found applications in climate studies. Using Monte Carlo simulations, Zhang *et al.* [2004] compared several methods for detecting trends in the magnitude of extreme values. They found that methods that specifically model trend in the parameters of extreme value distributions provide the highest power of detection of statistically significant trends. Wang *et al.* [2004] used covariates in their analyses of projected extreme ocean wave heights for the end of the 21st century. Kharin and Zwiers [2005] applied a similar model to general climate model simulated extremes to estimate the impact of anthropogenic climate change on climate extremes. All of these studies used the ML method for parameter estimation. Recently, Cunderlik and Ouarda [2006] developed the nonstationary approach to regional flood-duration-frequency (QdF) modeling.

[5] The method of maximum likelihood is efficient when the sample size is sufficiently large. Because of the complexity of the likelihood function, the ML estimates of the parameters for the GEV distribution can only be obtained through numerical methods. The ML method may diverge when sample size is small. To resolve the problems of divergence occurring in the numerical techniques used for ML, Martins and Stedinger [2000] suggest the use of a prior distribution for the shape parameter of the GEV model such that the most probable values of the parameter are included. This approach is similar to the quasi-Bayesian maximum likelihood estimator (QBML) of Hamilton [1991], which considers prior information about the parameters to eliminate the singularities associated with the ML method. The latter approach was successfully applied by Venkataraman [1997] for the solution of problems in finance. Morrison and Smith [2002] introduced a new method, named “mixed L moments: maximum likelihood,” to resolve the same singularity problem and to obtain unbiased estimators such as those produced by the ML method. This method consists of solving the equations of the maximum likelihood estimation method under the constraints given by the first L moment or the first two L moments. Through a simulation experiment, Morrison and Smith [2002] show that the estimators obtained with this method conserve the property of being unbiased and are characterized by a low variance. Dose and Menzel [2004] used a Bayesian approach to build nonparametric models when studying climate change effects in phenology.

[6] The majority of the models that consider dependence of parameters on covariates are based on the normality assumption of the variable. This assumption is not always verified, especially in the case of extreme values. Meanwhile, even when trends or any other causes of nonstationarity are eliminated, the resulting residual series is not

necessarily normal. Hydroclimatic extreme value variables are often characterized by a strong skewness.

[7] The objective of this study is to use the GEV distribution for quantile estimation in the presence of nonstationarity in the data series. To this end, we consider a nonstationary GEV model [Coles, 2001] in which the parameters are time-dependent or dependent on other covariates. We suggest the generalized maximum likelihood estimation method (GML) for parameter estimation [Martins and Stedinger, 2000]. The GML method integrates the prior information on the shape parameter. We present a generalization of this method in the case of a nonstationary GEV model. An additional advantage of the GML approach is that the numerical problems that may occur with the ML method when estimating parameters for short series can be avoided.

2. Nonstationary GEV Model

[8] The distributions of extreme values, introduced by Fisher and Tippett [1928], include three families: Gumbel, Fréchet, and Weibull. Jenkinson [1955] combined the three families into the generalized extreme values distribution (GEV) with a cumulative distribution function:

$$F_{\text{GEV}}(x) = \exp \left[- \left(1 - \frac{\kappa}{\alpha} (x - \mu) \right)^{1/\kappa} \right] \quad \kappa \neq 0$$

$$= \exp \left[- \exp \left(- \frac{(x - \mu)}{\alpha} \right) \right] \quad \kappa = 0 \quad (1)$$

where, $\mu + \alpha/\kappa \leq x < +\infty$ when $\kappa < 0$ (Fréchet), $-\infty < x < +\infty$ when $\kappa = 0$ (Gumbel) and $-\infty < x \leq \mu + \alpha/\kappa$ when $\kappa > 0$ (Weibull). $\mu (\in \mathbb{R})$, $\alpha (> 0)$ and $\kappa (\in \mathbb{R})$ are the location, the scale and the shape parameters, respectively.

[9] In the nonstationary case, the parameters are expressed as a function of covariates such as time: GEV ($\mu_t, \alpha_t, \kappa_t$) [Coles, 2001]. To ensure a positive value for the scale parameter, a transformation such that $\varphi_t = \log(\alpha_t)$ is used when estimating the parameters. We assume that the location parameter μ_t is a function of n_μ covariates $U = (U_1 \ U_2 \dots \ U_{n_\mu})'$. Let $\beta = (\beta_1 \ \beta_2 \dots \ \beta_{n_\mu})'$ be the vector of hyperparameters. In the case of linear dependence we have

$$\mu_t = U'(t)\beta = \sum_{i=1}^{n_\mu} \beta_i U_i(t) \quad (2)$$

For the scale parameter α_t , let $V = (V_1 \ V_2 \dots \ V_{n_\alpha})'$ be the vector of covariates. We have

$$\varphi_t = \log(\alpha_t) = V'(t)\delta = \sum_{i=1}^{n_\alpha} \delta_i V_i(t) \quad (3)$$

Where $\delta = (\delta_1 \ \delta_2 \dots \ \delta_{n_\alpha})'$ are the hyperparameters. The same applies to the shape parameter κ_t :

$$\kappa_t = W'(t)\gamma = \sum_{i=1}^{n_\kappa} \gamma_i W_i(t) \quad (4)$$

where, $W = (W_1 W_2 \dots W_{n_k})'$ are the covariates and $\gamma = (\gamma_1 \gamma_2 \dots \gamma_{n_k})'$ are the hyperparameters.

[10] For the nonstationary GEV model, the likelihood function for the sample $\underline{x} = \{x_1, \dots, x_n\}$ is:

$$L_n = \prod_{t=1}^n f(x_t; \mu_t, \varphi_t, \kappa_t) \quad (5)$$

where f is the probability density function (PDF) of the GEV distribution. For the sake of simplicity and for practical considerations, we restrict this study to the case of nonstationarity in the location and scale parameters, expressed as the following three nested models.

[11] 1. $GEV_0(\mu, \alpha, \kappa)$ is the classic model with all parameters being constant: $\mu_t = \mu, \alpha_t = \alpha$ et $\kappa_t = \kappa$. In this case $n_\mu = n_\alpha = n_\kappa = 1$ and $U_1 = V_1 = W_1 = 1$.

[12] 2. $GEV_1(\mu_t = \beta_1 + \beta_2 Y_t, \alpha, \kappa)$ is the homoscedastic model with location parameter linearly dependent on one covariate (Y_t). $n_\mu = 2, U(t) = (U_1(t) = 1 U_2(t) = Y_t), n_\alpha = n_\kappa = 1$ and $V_1 = W_1 = 1$.

[13] 3. In $GEV_2(\mu_t = \beta_1 + \beta_2 Y_t + \beta_3 Y_t^2, \alpha, \kappa)$ the location parameter is a quadratic function of the covariate Y_t . $n_\mu = 3, U(t) = (U_1(t) = 1 U_2(t) = Y_t U_3(t) = Y_t^2), n_\alpha = n_\kappa = 1$ and $V_1 = W_1 = 1$.

[14] 4. In $GEV_{11}(\mu_t = \beta_1 + \beta_2 Y_t, \alpha = \exp(\alpha_1 + \alpha_2 Y_t), \kappa)$ the location and scale parameters are function of the covariate Y_t . This model is recommended when the covariate is time, since trends are usually observed at the same time in the location and scale parameters. $n_\mu = 2, U(t) = (U_1(t) = 1 U_2(t) = Y_t), n_\alpha = 2, V(t) = (V_1(t) = 1 V_2(t) = Y_t), n_\kappa = 1$ and $V_1 = W_1 = 1$.

[15] Note that “nonstationary model” is a conventional name for models which parameters are function of covariates. Indeed, when covariates are not represented by the time, the studied process may be stationary. However, the term “nonstationary model” will be used for both cases. A more fundamental issue is that frequency analysis applications are quite different in the cases in which the covariate is the time argument and the cases in which the covariate is a time-varying stochastic process. In the former case, one can easily compute quantiles of the process of interest and examine how they vary over time. In the latter case, one can compute conditional distributions, given the value taken by the covariate.

3. Generalized Maximum Likelihood Estimators

[16] The vector of parameters θ to be estimated is, $\theta = (\mu, \alpha, \kappa)$ for the model GEV_0 , $\theta = (\beta_1, \beta_2, \alpha, \kappa)$ for the model GEV_1 , $\theta = (\beta_1, \beta_2, \beta_3, \alpha, \kappa)$ for the model GEV_2 and $\theta = (\beta_1, \beta_2, \delta_1, \delta_2, \kappa)$ for the model GEV_{11} . These models are considered to illustrate the estimation method. However, the methodology is general and can be applied to large range of nonstationary or dependent parameter models.

[17] In this section we present the generalized maximum likelihood method for the estimation of the parameters of nonstationary GEV model. The GML is based on the maximum likelihood (ML) estimator. In the following, we first introduce ML estimators for the three models. We then present the GML estimators.

[18] For a sample of n observations $\underline{x} = (x_1, \dots, x_n)$, the maximum likelihood estimators of the nonstationary GEV

model parameters can be determined by maximizing the likelihood function, given by the general form [Coles, 2001]

$$L_n(\underline{x}; \mu_t, \alpha_t, \kappa_t) = \prod_{t=1}^{n_1} \frac{1}{\alpha_t} \exp \left\{ - \left[1 - \kappa_t \left(\frac{x_t - \mu_t}{\alpha_t} \right) \right]^{-1/\kappa_t} \right\} \\ * \left[1 - \kappa_t \left(\frac{x_t - \mu_t}{\alpha_t} \right) \right]^{-\left(1 - \frac{1}{\kappa_t}\right)} * \prod_{t=n_1+1}^n \frac{1}{\alpha_t} \\ \cdot \exp \left\{ - \left(\frac{x_t - \mu_t}{\alpha_t} \right) \right\} * \exp \left\{ - \exp \left[- \left(\frac{x_t - \mu_t}{\alpha_t} \right) \right] \right\} \quad (6)$$

where n_1 is the number of observations such as $\kappa_t \neq 0$. For all models considered in this paper, nonstationarity is related to the location parameter and scale parameter. We then have: $\kappa_t = \kappa$ is a constant. When $\kappa \neq 0$, we also have $n_1 = n$, and the log likelihood function becomes

$$l_n(\underline{x}; \mu_t, \alpha_t, \kappa) = -n \log(\alpha_t) - \sum_{t=1}^n \left[1 - \kappa \left(\frac{x_t - \mu_t}{\alpha_t} \right) \right]^{1/\kappa} \\ - \sum_{t=1}^n \left(1 - \frac{1}{\kappa} \right) \log \left[1 - \kappa \left(\frac{x_t - \mu_t}{\alpha_t} \right) \right] \quad (7)$$

In practice, it is easier to maximize the log likelihood function. The ML estimators are the solution of an equation system formed by setting to zero the partial derivatives of l_n with respect to each parameter.

[19] For the GEV_1 model the ML estimators of the parameters $(\beta_1, \beta_2, \alpha, \kappa)$ are the solution of the following system:

$$\sum_{t=1}^n \frac{1 - \kappa - z_t^{1/\kappa}}{z_t} = 0 \\ \sum_{t=1}^n t \frac{1 - \kappa - z_t^{1/\kappa}}{z_t} = 0 \\ -n + \sum_{t=1}^n \left[\frac{1 - \kappa - z_t^{1/\kappa}}{z_t} \left(\frac{x_t - \mu_t}{\alpha} \right) \right] = 0 \\ \sum_{t=1}^n \left\{ \ln(z_t) \left[1 - \kappa - z_t^{1/\kappa} \right] + \frac{1 - \kappa - z_t^{1/\kappa}}{z_t} \kappa \left(\frac{x_t - \mu_t}{\alpha} \right) \right\} = 0 \quad (8)$$

where $z_t = \left[1 - \frac{\kappa}{\alpha} (x_t - \mu_t) \right]$.

[20] Numerical methods, such as the Newton-Raphson method, must be used to solve this system. Similarly, an equation system equivalent to (8) can be obtained for the GEV_2 (respectively, GEV_{11}) models, with the fifth equation corresponding to the β_3 (respectively, δ_2) parameter.

[21] Under certain regularity conditions, the ML estimators have the desired asymptotic properties. These conditions are not verified, however, when the shape parameter $\kappa \neq 0$, since the support of the distribution depends on the parameters [Smith, 1985]. In the classic case (GEV_0), this problem generally leads to estimators with a very high variance. The ML estimator properties for each of the three models will be examined in section 4. Standard error and confidence interval approximations can be obtained, as in the classic case, by a numerical evaluation of the Fisher information matrix. Another problem associated with the

ML method when used with small sample sizes, is that the numerical resolution of the ML system ((8) for GEV1 model) can lead to physically impossible estimators of the parameters, and to very high quantile estimator variances.

[22] The GML method is based on the same principle as the ML Method with an additional constraint on the shape parameter to eliminate potentially invalid values of this parameter. A prior distribution of κ , in the case of the hydrometeorological series, was introduced by *Martins and Stedinger* [2000] based on practical considerations. *Martins and Stedinger* [2000] presented the GML method for the GEV0 model, using a Beta distribution as prior for the shape parameter κ : $\pi_{\kappa}(\kappa) = \text{Beta}(u = 6, v = 9)$. This distribution is centered on the value -0.1 and has the interval $[-0.5, +0.5]$ as support. This method can be generalized to the nonstationary GEV model by using a similar prior for the shape parameter and resolving the ML system generated under this constraint (equation system (8) for the GEV1 model). The GML parameter estimators are the solution to the following optimization problem:

$$\begin{cases} \max_{\theta} L_n(\underline{x}; \theta) \\ \kappa \sim \text{Beta}(u, v) \end{cases} \quad (9)$$

This is equivalent to maximizing the posterior distribution of the parameters conditionally to the data:

$$\pi(\theta|\underline{x}) \propto L_n(\underline{x}|\theta)\pi_{\kappa}(\kappa) \quad (10)$$

where L_n is given by the equation (6).

[23] As indicated by *Martins and Stedinger* [2000], the GML method is a particular case of the Bayesian approach, where the prior distribution is only specified for the shape parameter. An important advantage, of the use of the GML method, is the possibility to integrate any additional information, such as historical and regional information, to define the prior distributions. This point was well discussed by *Reis and Stedinger* [2005].

[24] The GML parameter estimator corresponds to the mode of the posterior distribution, which is not explicitly known, and can be computed by numerical methods [*Martins and Stedinger*, 2000]. An alternative is the use of simulation methods such as Monte Carlo Markov Chain methods (MCMC). The MCMC approach allows to determine the empirical posterior distribution of the parameter vector, and to deduct the marginal distributions of the parameters and their characteristics. The GML estimators are thus the modes of the empirical marginal distributions generated by the MCMC method.

4. Parameter and Quantile Computation via MCMC

[25] The MCMC method constitutes an alternative to the numerical methods, especially in Bayesian statistical analysis. The basic idea of the MCMC method is, for each parameter, to construct a Markov chain with the posterior distribution being a stationary and ergodic distribution. After running the Markov chain, of size N , for a given burn-in period, N_0 , one obtains a sample from the posterior distribution $\pi(\theta|\underline{x})$. One popular method for constructing a Markov chain is via the Metropolis-Hastings (MH) algo-

rithm [*Metropolis et al.*, 1953; *Hastings*, 1970]. For the GML method, we simulated realizations from the posterior distribution by way of a single-component MH algorithm [*Gilks et al.*, 1996]. Each parameter was updated using a random walk Metropolis algorithm with a Gaussian proposal density centered at the current state of the chain. Some methods to assess the convergence of MCMC methods make it possible to determine the length of the chain and the burn-in time such as Raftery and Lewis and subsampling methods [*El Adlouni et al.*, 2006]. In all cases, the convergence methods indicated that the Markov chains converged within some iteration. In this study, we considered chains of size $N = 15000$ and a burn-in period of $N_0 = 8000$ runs. In every case, a sample of $N - N_0 = 7000$ values is collected from the posterior of each of the elements of θ . The GMLE corresponds to the mode of the empirical posterior distribution obtained from the histogram of $N - N_0$ values generated by the MCMC algorithm.

[26] The MCMC algorithm produces also the conditional quantile distribution for an observed value, y_0 , of the covariate Y_t . Indeed, for each iteration i of the MCMC algorithm, $i = 1, \dots, N$, the quantiles with nonexceedance probability p , $x_{p,y_0}^{(i)}$ corresponding to the parameter vector $(\mu_{y_0}^{(i)}, \alpha_{y_0}^{(i)}, \kappa^{(i)})$, are computed using the inverse of the cumulative distribution function of the GEV distribution:

$$x_{p,y_0}^{(i)} = \left(\mu_{y_0}^{(i)} + \frac{\alpha_{y_0}^{(i)}}{\kappa^{(i)}} \left[1 - (-\log(p))^{\kappa^{(i)}} \right] \right) \quad (11)$$

Where $\mu_{y_0}^{(i)}, \alpha_{y_0}^{(i)}$ are the position and scale parameters conditional on the particular value y_0 of Y_t . We have: $\mu_{y_0}^{(i)} = \mu^{(i)}, \alpha_{y_0}^{(i)} = \alpha^{(i)}$ for the GEV0 model; $\mu_{y_0}^{(i)} = \beta_1^{(i)} + \beta_2^{(i)} y_0$ for the GEV1 model and $\mu_{y_0}^{(i)} = \beta_1^{(i)} + \beta_2^{(i)} y_0 + \beta_3^{(i)} y_0^2$ for the GEV2 model. For these models $\alpha_{y_0}^{(i)} = \alpha^{(i)}$. For the GEV11 model $\mu_{y_0}^{(i)} = \beta_1^{(i)} + \beta_2^{(i)} y_0$ and $\alpha_{y_0}^{(i)} = \exp(\delta_1^{(i)} + \delta_2^{(i)} y_0)$. Several statistical characteristics of the conditional quantile distribution, such as the mean, the mode or intervals of credibility, can be determined from the values $x_{p,y_0}^{(i)}, i = N_0, \dots, N$.

5. Simulation Study

[27] In order to study and compare the estimation parameter methods for each of the three models (GEV0, GEV1, GEV2, and GEV11), we considered the case of a time-dependent location parameter ($Y_t = t$). The quantiles, $x_{p,n}$, are computed conditionally to $Y_t = n$, which corresponds to an update of the parameter distribution. We considered the same parameters used by *Martins and Stedinger* [2000] to compare the GML method, the ML method, the method of moments (MM), and the probability-weighted moments method (PWM). We are interested in the case of positive skewness with the following values of the shape parameter: $\kappa = -0.1 \quad \kappa = -0.2 \quad \kappa = -0.3$. The main objective of the simulation study is to compare the performance of the estimation methods presented above for various skewness values. The parameters defining the nonstationarity were chosen to have weak trends, which often corresponds to the conditions observed with hydrometeorological series. For the GEV1 model two cases were considered, in order to test the sensitivity of simulation results to the values of parameters. The first one (case 1) corresponds to $\beta_1 = 0$ and $\beta_2 =$

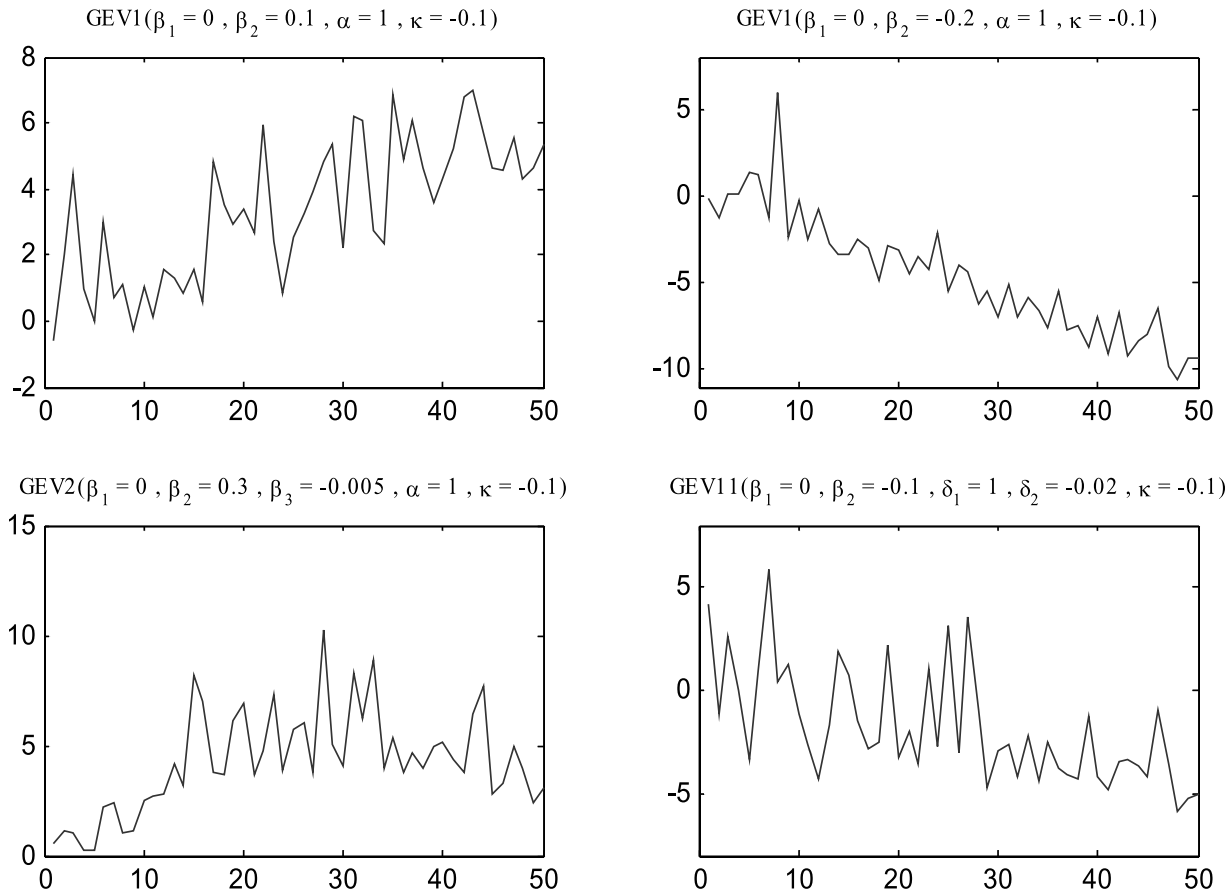


Figure 1. Series generated by the GEV1, GEV2, and GEV11 models.

0.1 and the second case (case 2) $\beta_1 = 0$ and $\beta_2 = -0.2$. For the GEV2 model $\beta_1 = 0, \beta_2 = 0.3$ and $\beta_3 = -0.005$ and for the GEV11 model $\beta_1 = 0, \beta_2 = -0.1, \delta_1 = 1$ and $\delta_2 = -0.02$. For models with fixed scale parameter: $\alpha = 1$. Examples of the generated series are presented in Figure 1.

[28] The Monte Carlo simulation study was carried out to compare the ML and GML methods. The bias and the root-mean-square error (RMSE) were computed for each quantile of nonexceedance probabilities $p = 0.5, 0.8, 0.9, 0.99$ et 0.999 (corresponding to return periods 2, 5, 10, 100 and 1000 years in the classic case). The bias and RMSE were calculated for $R = 1000$ samples with a sample size of $n = 50$ generated by each of the studied models.

5.1. GEV0 Model

[29] For the classic GEV0 model, the comparison was made for three skewness values corresponding to $\kappa = -0.1, \kappa = -0.2,$ and $\kappa = -0.3$. The location and scale parameters were fixed to $\mu = 0$ and $\alpha = 1$. Table 1 presents the bias and the RMSE of the nonexceedance probability quantiles obtained with the GEV0 model.

[30] Results in Table 1 show that for the low skewness value ($\kappa = -0.1$), the GML method provides the best results for all quantiles. The prior distribution mode used in the GML method for the shape parameter is equal to -0.1154 . This choice gave more weight to the central value of the prior distribution which explains the negative bias obtained with the larger skewness values ($\kappa = -0.2$ and $\kappa = -0.3$). Concerning the ML method, Table 1 supports the conclusions made in the literature: High RMSE values are due to

the large ML estimator variance, caused by a few aberrant values of the ML estimation of the shape parameter κ .

5.2. GEV1 Model

[31] As mentioned above, the covariate used during the simulations studies was time $Y_t = t$. In order to study the

Table 1. GEV0 Model: Bias and RMSE of Quantiles Estimated by the ML and GML Methods

p	Bias		RMSE	
	ML	GML	ML	GML
	$\kappa = -0.1$			
0.5	0.02	0.01	0.35	0.17
0.8	-0.03	0.05	0.44	0.33
0.9	-0.05	0.04	0.45	0.45
0.99	0.02	0.11	1.86	0.94
0.999	0.71	0.22	6.01	1.60
	$\kappa = -0.2$			
0.5	-0.01	0.05	0.20	0.24
0.8	-0.02	-0.03	0.35	0.33
0.9	-0.01	-0.05	0.57	0.42
0.99	0.57	-0.17	3.31	1.20
0.999	1.72	-0.37	14.35	3.53
	$\kappa = -0.3$			
0.5	-0.04	-0.01	0.17	0.20
0.8	-0.12	-0.04	0.35	0.39
0.9	-0.16	-0.07	0.75	0.64
0.99	0.19	-0.23	4.44	2.48
0.999	1.96	-0.42	21.08	7.83

Table 2. GEV1 Model (Case 1): Bias and RMSE of Quantiles Estimated by the ML and GML Methods^a

<i>p</i>	Bias		RMSE	
	ML	GML	ML	GML
$\kappa = -0.1$				
0.5	0.06	0.01	0.41	0.39
0.8	0.04	0.03	0.47	0.50
0.9	-0.02	0.03	0.56	0.56
0.99	-0.17	0.05	1.58	0.85
0.999	-0.14	0.12	4.17	1.36
$\kappa = -0.2$				
0.5	0.01	0.02	0.45	0.30
0.8	0.02	0.05	0.53	0.51
0.9	0.03	0.06	0.73	0.73
0.99	0.26	-0.11	3.04	2.08
0.999	1.74	-0.17	11.33	5.24
$\kappa = -0.3$				
0.5	0.07	0.03	0.56	0.36
0.8	0.04	0.04	0.66	0.59
0.9	-0.03	0.04	0.88	0.83
0.99	-0.64	-0.12	4.10	2.44
0.999	-1.34	-0.61	17.95	7.06

^aFor case 1, $\beta_2 = 0.1$.

sensitivity of simulation results to the value of trend parameter used for the GEV1 model, we consider two cases. However, we think that, for the GEV distribution, results are more sensitive to the value of the shape parameter. Two case of trend parameter are considered for the GEV 1 model. For case 1: $\beta_1 = 0, \beta_2 = 0.1, \alpha = 1$ and the shape parameter represented three positive skewnesses.

[32] Table 2 reports the bias and the RMSE values for each quantile estimate for the GEV1 model (case 1). Results demonstrate that the GML method performed better than the ML method especially for quantiles corresponding to high nonexceedance probabilities. For higher probabilities, the

Table 3. GEV1 Model (Case 2): Bias and RMSE of Quantiles Estimated by the ML and GML Methods^a

<i>p</i>	Bias		RMSE	
	ML	GML	ML	GML
$\kappa = -0.1$				
0.5	-0.26	-0.01	1.32	0.11
0.8	-0.21	0.03	1.31	0.22
0.9	-0.34	0.06	2.38	0.37
0.99	-0.79	0.25	5.13	1.79
0.999	-0.84	0.68	7.94	3.27
$\kappa = -0.2$				
0.5	-0.15	0.03	1.61	0.10
0.8	-0.78	0.03	1.53	0.21
0.9	-0.72	0.15	1.56	0.38
0.99	-0.83	-0.69	4.69	1.49
0.999	-1.34	-1.02	18.01	7.19
$\kappa = -0.3$				
0.5	-0.77	0.08	1.42	0.13
0.8	-0.75	-0.05	1.61	0.38
0.9	-0.77	-0.21	2.09	1.42
0.99	-1.06	-0.79	7.52	4.76
0.999	-1.35	-1.22	25.08	12.52

^aFor case 2, $\beta_2 = -0.2$.

Table 4. GEV2 Model: Bias and RMSE of Quantiles Estimated by the ML and GML Methods

<i>p</i>	Bias		RMSE	
	ML	GML	ML	GML
$\kappa = -0.1$				
0.5	-0.06	0.01	0.98	0.56
0.8	-0.71	0.04	1.02	0.66
0.9	-0.76	0.07	1.09	0.77
0.99	-0.99	0.13	1.96	1.30
0.999	-1.12	0.18	4.63	2.12
$\kappa = -0.2$				
0.5	-0.81	0.02	1.22	0.64
0.8	-0.79	0.05	1.23	0.80
0.9	-0.80	0.06	1.30	0.97
0.99	-0.93	-0.11	2.83	1.94
0.999	-1.79	-0.17	8.93	3.73
$\kappa = -0.3$				
0.5	-0.83	0.27	1.47	0.97
0.8	-0.92	0.48	1.46	1.38
0.9	-0.81	0.61	1.87	1.86
0.99	-1.57	1.42	3.87	3.48
0.999	-3.69	2.87	12.62	8.54

ML estimator produced a negative bias and high RMSE values. Compared to the GEV0 model, the GML estimators of the GEV1 model parameters have a smaller bias (in absolute value). For the second case of GEV1 model, $\beta_1 = 0, \beta_2 = -0.2, \alpha = 1$, and the shape parameter represented three positive skewnesses.

[33] Table 3 reports the bias and the RMSE values for each quantile estimate of the GEV1 model (case 2). This case confirms results obtained for case 1. The GML method leads to better estimates than the ML method. Note that for this case RMSE values are higher than those obtained for case 1 for all quantiles and the bias values for the GML estimators are negative but small in absolute value.

5.3. GEV2 Model

[34] The GEV2 model typifies the case where the location parameter is a quadratic function of a covariate, represented by time in this case. This case demonstrates the flexibility of the nonstationary GEV model for studying different types of dependence structure.

[35] Results obtained with the GEV2 model show that the GML method leads to small bias and RMSE especially for small skewness (Table 4). The use of a quadratic dependence structure reduces the impact of the central value of the shape parameter prior distribution used in the GML method. The bias of the ML estimators is negative for all quantiles and skewness values. It is also relatively large (in absolute value) compared to the GML method. However, the variance of the ML estimators is smaller than that obtained with the GEV0 and GEV1 models.

5.4. GEV11 Model

[36] The last model, GEV11, is also a generalization of the GEV1 model. For this model, location and scale parameters are linear functions of the same covariate (time in this case). Parameters considered in this study are: $\beta_1 = 0, \beta_2 = -0.1, \delta_1 = 1$, and $\delta_2 = -0.02$. As in all cases the sensitivity of results is tested for three shape parameter

Table 5. GEV11 Model: Bias and RMSE of Quantiles Estimated by the ML and GML Methods

p	Bias		RMSE	
	ML	GML	ML	GML
		$\kappa = -0.1$		
0.5	-0.06	-0.05	2.04	0.25
0.8	-0.27	-0.03	3.18	0.63
0.9	-0.55	0.12	4.33	1.12
0.99	-0.79	0.14	6.31	3.32
0.999	-1.27	0.62	11.31	6.62
		$\kappa = -0.2$		
0.5	-0.45	-0.25	1.73	1.04
0.8	-1.19	-0.34	2.29	1.83
0.9	-2.29	-0.33	4.30	3.84
0.99	-2.98	-1.56	9.83	7.65
0.999	-4.98	-2.78	18.93	12.71
		$\kappa = -0.3$		
0.5	0.12	-0.36	2.46	1.47
0.8	-0.08	-0.42	2.26	2.13
0.9	-0.81	-0.83	4.35	3.16
0.99	-1.58	-1.36	12.87	7.38
0.999	-2.49	-1.68	22.62	13.24

values (-0.1, -0.2, and -0.3). Empirical studies on nonstationary models indicate that it is preferable to represent the nonstationarity in both location and scale parameters. Indeed, for observed data, a trend in the location is often accompanied by a reduction or increase in the variance.

[37] Results obtained with the GEV11 model show that the GML method leads to a high bias for all skewness values especially for quantiles with high probability of nonexceedance (Table 5). The increase in RMSE of the estimators in this case, compared to the GEV1 model, is due to the bias. However, when compared to the ML method, the GML approach gives good results for all skewness values.

6. Annual Maximal Precipitations and the SOI Index

[38] We applied the models presented above to a series $\underline{X} = (x_1, \dots, x_n)$ of annual maximum precipitation (mm), recorded at the Randsburg station in California (station 047253) with 51 years of record. The latitude of the station is 35.3700, its longitude 117.650 and the period of record is 1949–1999. Figure 2 illustrates the geographic location of the Randsburg station. Located in the southern part of California, precipitation in this station should be strongly affected by the El Niño phenomenon.

[39] In this application of the nonstationary GEV models, the main objective was to study the conditional distribution of the annual maximal precipitation (X) as a function of the Southern Oscillation Index (SOI). The SOI is computed using monthly mean sea level pressure anomalies at Tahiti (T) and Darwin (D). Strongly negative values of SOI are observed during an El Niño, around 0 on a normal year and strongly positive during a La Niña. The correlation coefficient between the annual maximal precipitations X and the SOI is $\rho = -0.60$ (Figure 3).

[40] We observe a significant negative correlation between X and the SOI. Figure 4 shows that the extreme

values of X correspond to low SOI values. Each of the three GEV models, presented in section 2, is used to study the conditional distribution of the annual maximal precipitation according to the SOI index.

[41] The parameters, of GEV0, GEV1, and GEV2 models, were estimated by the ML and the GML methods. However, only the results of the GML method are reported herein. Figure 5 illustrates the convergence of the $N = 15000$ iterations of the Metropolis-Hastings algorithm used for the estimation of the GEV0 model parameters. After running the MH algorithm for a burn-in period of $N_0 = 8000$ runs, samples were generated from the posterior distribution. The histograms of the last $N - N_0$ iterations represent the empirical posterior distributions of the parameters and allow the determination of all theoretical distribution properties (Figure 6). The GML estimators correspond to the modes of the marginal distributions, listed in Table 6 with the maximized log likelihood l_n^* values.

[42] The GEV0 model is a particular case of the GEV1 model, which itself is a particular case of the quadratic dependence GEV2 model. The most general model is usually the best model to represent data variance. However, when the difference between two models is not evident it is preferable to use the simplest model in order to respect the parsimony principle. Indeed, for nonstationary models, the use of covariates leads to a better description of the process that generates data but the number of parameters to be estimated increases. For small and moderate samples, this leads to a large variance and consequently and an increased uncertainty in quantile estimation.

[43] A simple method to compare the validity of a model M_1 against another model M_0 , such as $M_0 \subset M_1$, is to use the deviance statistic defined by [Coles, 2001]:

$$D = 2\{l_n^*(M_1) - l_n^*(M_0)\} \tag{12}$$

where $l_n^*(M)$ is the maximized log likelihood function of model M . Large values of D indicate that model M_1 is more

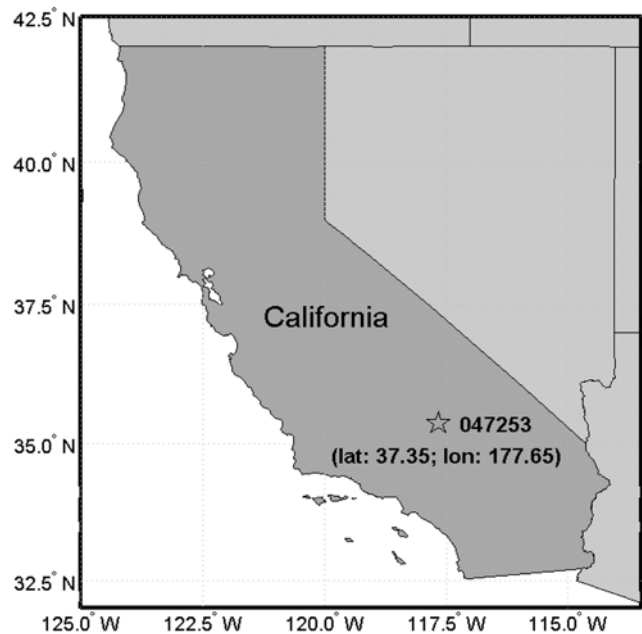


Figure 2. Geographic location of the Randsburg station in California.

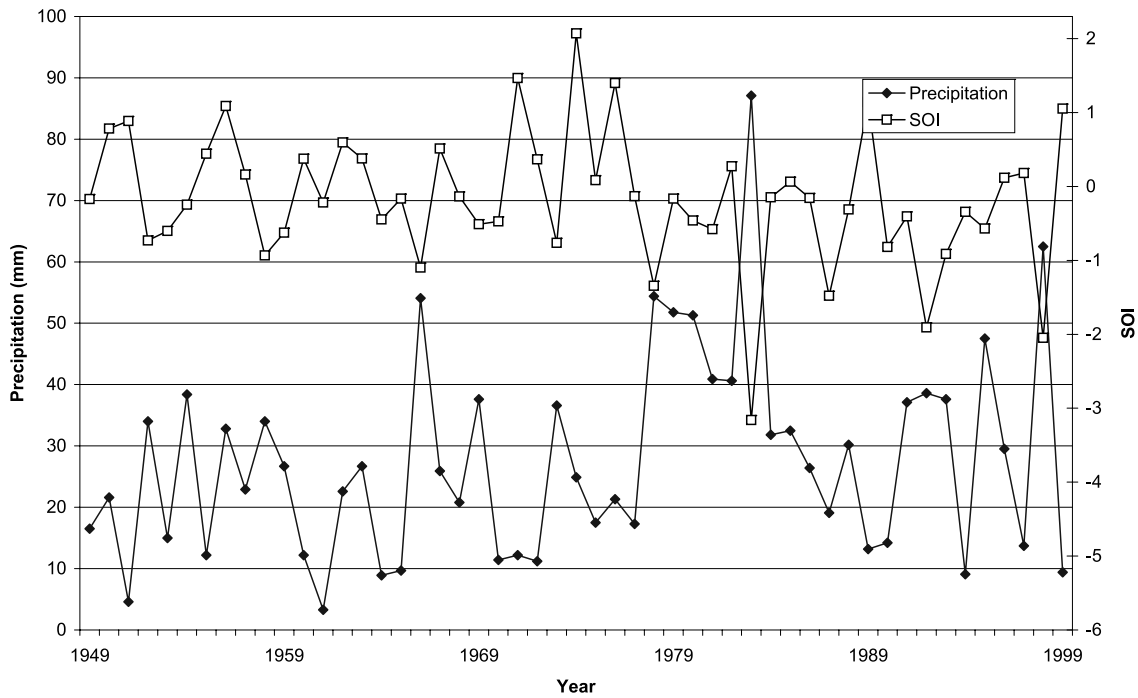


Figure 3. Observed annual maximal precipitation and the SOI series.

adequate and explains more of the data variation than model M_0 . The statistic D is distributed according to a chi-square (χ^2_ν) distribution. The parameter ν is the difference between the dimensions (number of parameters) of the M_1 and M_0 models. Values of D greater than the quantiles of the χ^2_ν distribution for a particular confidence level, are considered significant thus model M_1 is better than model M_0 .

[44] The models studied in this work, can also be compared in a Bayesian framework using the posterior predictive distributions. Simulations from these distributions can be compared with respect to goodness of fit or proposed inferences [Gelman et al., 1995]. The posterior predictive p value and conditional p value are also emerging as popular measures of model fit [Bayarri and Berger, 2000;

Aitkin et al., 2005]. It would be interesting to study the power of all these techniques within a nonstationary case.

[45] There is a significant difference between the GEV0 and the GEV1 models since $D = 6.2$ is bigger than the 0.95 quantile of the χ^2_1 distribution ($\Pr(\chi^2_1 \leq 6.2) = 0.9872$). The GEV1 model led to a maximized log likelihood value of $l_n^*(\text{GEV}_1) = -206.86$. In the case of quadratic dependence in the location parameter μ , the maximized log likelihood becomes $l_n^*(\text{GEV}_2) = -204.71$. The deviance statistic for comparing these two models is therefore $D = 4.3$. This value is large when compared to the χ^2_1 distribution ($\Pr(\chi^2_1 \leq 4.3) = 0.9619$), implying that the quadratic model (GEV2) explains a substantial amount of the variation in the data, and is likely to best represent the dependence between the annual maximal precipitation and the SOI index.

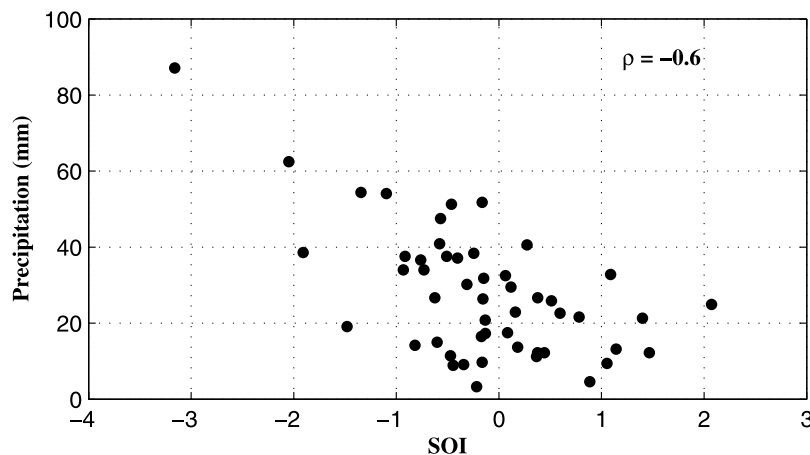


Figure 4. Observed annual maximal precipitation and corresponding SOI value.

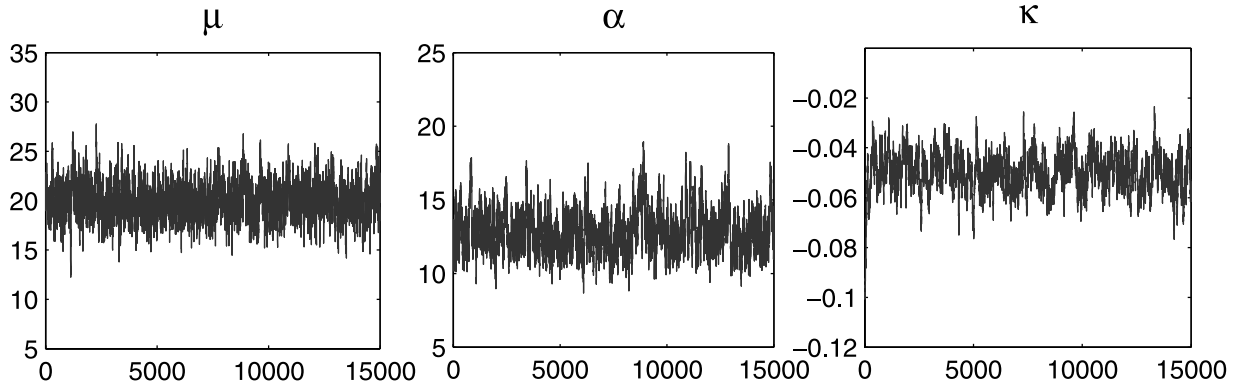


Figure 5. Convergence of the $N = 15,000$ iterations of the Metropolis-Hastings algorithm for the estimation of the GEV0 model parameters by the GML method.

[46] The GEV1 model can also be compared to the GEV11 model, by the deviance statistic, since the first one is a special case of the second. Log likelihood functions are given in Table 6 and the deviance statistic $D = 2\{l_n^*(\text{GEV}_{11}) - l_n^*(\text{GEV}_1)\} = 33.08$. It is clear that there is a significant difference between GEV11 and GEV1. Indeed, this value is large when compared to χ_1^2 distribution ($\Pr(\chi_1^2 \leq 33.08) = 0.9999$), implying that the GEV11 model is more adequate to represent data than the GEV1 model.

[47] The difference between the three models can also be demonstrated by comparing the quantiles estimated by each model. Quantiles and their credible intervals are calculated using equation (11). Figure 7 illustrates the conditional medians for various values of the SOI and the 95% credible intervals estimated for the GEV0 and GEV1 models. Figure 8 presents similar results for the GEV0 and GEV2 models.

[48] Table 7 presents, in more detail, the exact GML estimator values of the median and the 95% credible intervals for the following values of the SOI: -3.16 , 0.04 and 2.04 . These values correspond to the minimum observed value, a central value, and the maximum observed value of the SOI index.

[49] Results show that the difference is greater for negative values of SOI which correspond to extreme values in the annual maximal precipitation data. Indeed, the median estimated by the quadratic model, GEV2, can be three times greater than that estimated by the classic model, GEV0. Results of the comparison test with the deviance statistic indicate that the GEV2 model is more adequate to represent the precipitation data. Thus the use of either simplified model (GEV0 or GEV1) could lead to a significant under estimation of the median in some cases. Indeed, the GEV0 model leads to an under estimation of the median in the case of negative SOI values, while the GEV1 leads to an under estimation of the median for large SOI values. On the other side, overestimation can result of the use of the GEV0 model with large positive values of SOI.

[50] As mentioned above, trend and dependence on covariates, are often characterized by a change in the position and/or scale parameters. The deviance statistic shows that GEV11 is more adequate to represent data than the GEV1 model. Point estimates of quantiles given by the GEV11 model are equivalent to those obtained by GEV1 for low and mean values of SOI (Figure 9). However for a high

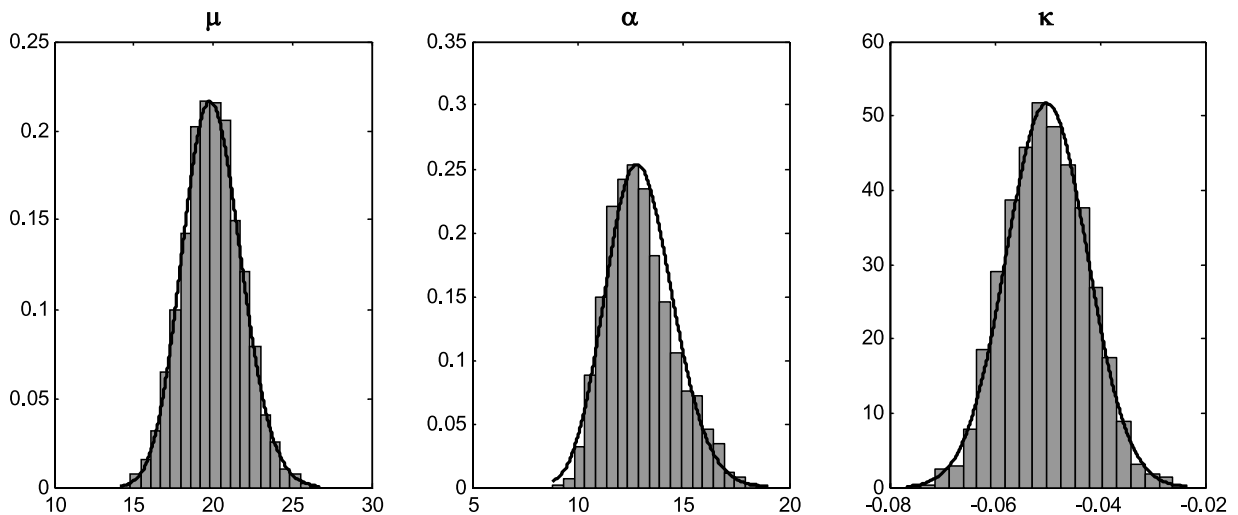


Figure 6. Histograms of the posterior distributions of the GEV0 model parameters obtained from the last 7000 iterations of the MCMC algorithm.

Table 6. Maximized Log Likelihood Function and GML Parameter Estimators for Each Model

	l_n^*	β_1	β_2	$\beta_3(\text{GEV}_2)$ $\delta_1(\text{GEV}_{11})$	α	$\delta_2(\text{GEV}_{11})$	κ
GEV ₀	-209.96	19.52	-	-	12.36	-0.05	
GEV ₁	-206.86	18.89	-9.92	-	12.21	-0.07	
GEV ₂	-204.71	16.57	-10.61	3.03	12.14	-0.06	
GEV ₁₁	-188.17	23.02	-4.57	2.17	-0.55	-0.06	

value of SOI, median estimates for GEV11 are three times larger than GEV1 estimates (Table 7). Another important difference between these two models, concerns the range of credible intervals. For the GEV11 model, credible intervals are larger than GEV1 for high and low values of SOI. However, for central values, GEV11 estimates are smaller. Consequently, the precision of the estimation is also function of the covariate. Since very few observations are available in the case of low values of SOI, little information is available on the dependence between parameters and covariates. Consequently, the GEV11 credibility interval with in this case is large.

7. Conclusions and Recommendations

[51] In this study, we presented the nonstationary GEV model which can be used efficiently to describe data variance. The focus was on nonstationarity (dependence on covariates) in the location and scale parameters of the GEV distribution. Several other models are available in the literature to describe random variables in nonstationary cases but are based on the hypothesis of normality. In the case of extreme value variables, the nonstationary GEV model is a commonly accepted model to describe nonstationarity. The models presented in this study correspond to the classic stationary GEV case, the case in which there is a linear trend in the location parameter, the case where the

location parameter is a quadratic function of the covariate and the case with linear trend in both location and scale parameters.

[52] Parameter estimation for these models is generally carried out using the maximum likelihood estimation method. The resulting estimators have good asymptotic properties under certain regularity conditions that are, in general, not verified by the GEV model. For small-size samples, maximum likelihood estimators may have a very large variance. In addition to efficiency problems, the numerical resolution of the maximum likelihood equations can lead to convergence problems and can, in some cases; result in solutions that are not physically acceptable. In order to resolve numerical problems, the generalized maximum likelihood method introduced by *Martins and Stedinger* [2000] assumes a prior distribution for the shape parameter which eliminates impossible solutions. We extended the GML method for the estimation of parameters to the nonstationary case, using the same prior distribution for the shape parameter as in the classic stationary GEV case. The GML method is itself a special case of the Bayesian approach, where an informative prior distribution is specified for the shape parameter. An important issue associated with the Bayesian approach is the selection of the prior distributions. For the nonstationary GEV model, further research should focus on the noninformative prior case in order to study the sensitivity of the estimators with respect to the choices of the parameters of the MCMC methods.

[53] The Monte Carlo Markov chains (MCMC) method was used for estimator calculations in the case of the GML method. The MCMC methods allow to obtain the posterior distributions of parameters and quantiles and thus to deduce the credible intervals for the inference. The comparison of the estimation methods ML and GML, with a simulation experiment shows that, in all cases, the GML method produces the best results with respect to bias and root-mean-square error (RMSE). In the case of the classical stationary GEV model, the GML method led to negative

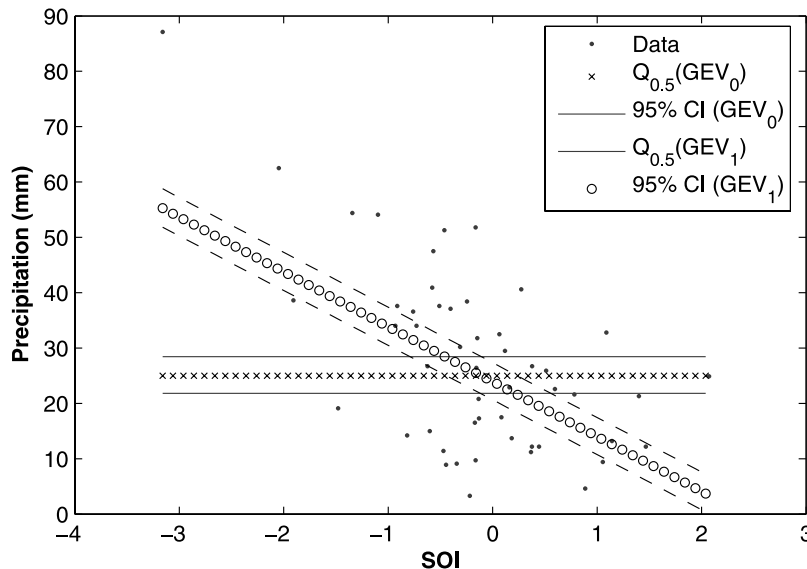


Figure 7. GML estimators of the median and 95% credible intervals conditional upon values of the SOI, obtained by the GEV0 and GEV1 models.

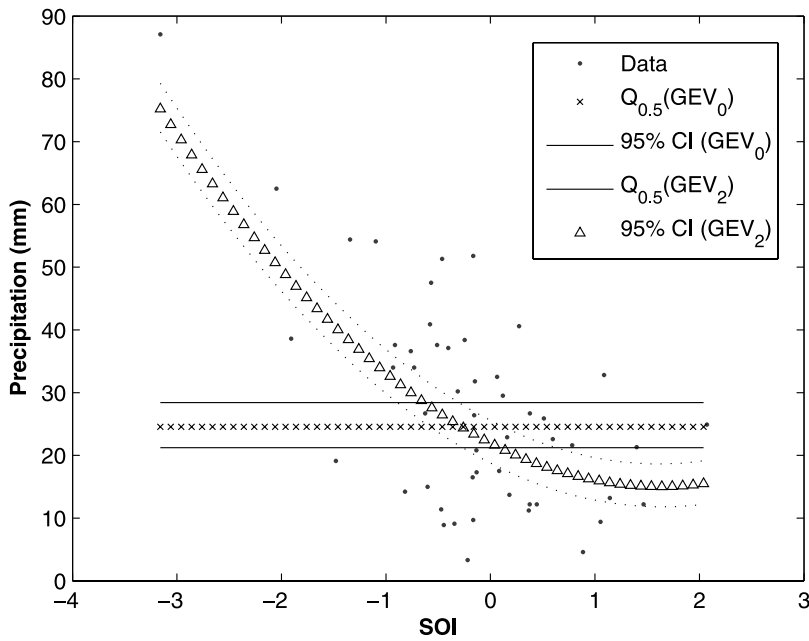


Figure 8. GML estimators of the median and 95% credible intervals conditional upon values of the SOI, obtained by the GEV0 and GEV2 models.

bias values for high skewness cases. This can be explained by the fact that the prior distribution of the shape parameter is centered on -0.1 . When the GML method is applied in practice, it is important to take into consideration any additional information, such as historical and regional information, to define the prior distributions [Reis and Stedinger, 2005].

[54] The three models considered in the simulation experiment (classic model GEV0, linear trend model GEV1, and quadratic dependence structure model GEV2) were used to estimate quantiles of the annual maximum precipitation at the Randsburg station in California, conditional on the SOI index. The comparison of these models using a test based on the deviance statistic shows that the GEV2 model most adequately represents the data variance. This example demonstrates the importance of using the nonstationary model to take into consideration the dependencies that may exist between the variables of interest and other covariates in order to improve the estimation quality. It was observed, in the case of the Randsburg station, that the median GEV2 model estimator conditional on a low SOI index value can reach three times the median estimation value of the GEV0 model.

[55] The nonstationary GEV model presented in this paper constitutes an efficient tool to take into consideration the dependencies between extreme value random variables or the temporal evolution of the climate. For instance, such tool can be of high significance for the design of hydraulic structures with consideration of changes occurring in the Earth’s climate. The design event frequency should also take into consideration the regime that is expected toward the end of the life time of the structure and not only at the time of the design of the structure. In the case of design problems, the covariate to be considered is the time. The nonstationary model presented in this paper can also be useful for management purposes: For example it is possible

to adjust flood plain limits to the current state of some predictors such as relevant low-frequency climate oscillation indices (such as the SOI index considered in section 6). Flooding risk levels can then be reestimated more efficiently on a yearly basis. The nonstationary approach could also be used for the solution of the problem of hydropower capacity estimation [Ouarda et al., 1997]. Hydrogeneration companies could then set their reliable delivery levels on a yearly basis with consideration of the current state of the climate and by using the appropriate covariates as predictors. In the case of management problems, the covariates to be considered are hence climate indices.

[56] In this paper, we only considered the case where the location parameter of the GEV distribution depends on one covariate. Other nonstationary cases warrant study. Further studies can focus on other statistical distributions and different nonstationarity structures, such as trends in the variance of the series (scale parameter). The GML estimation method is presented in a general manner and can be used in other nonstationary conditions. Future work can also focus on the development of a new framework for risk

Table 7. GML Estimators of the Median, Conditional on Three Values of SOI, and 0.95 Credible Intervals

	SOI		
	-3.16	0.04	2.04
GEV ₀	24 (21–28)	24 (21–28)	24 (21–28)
GEV ₁	54 (51–58)	23 (19–27)	4 (0.5–7)
GEV ₂	77 (72–82)	21 (18–24)	17 (15–22)
GEV ₁₁	56 (47–67)	26 (23–28)	14 (12–17)

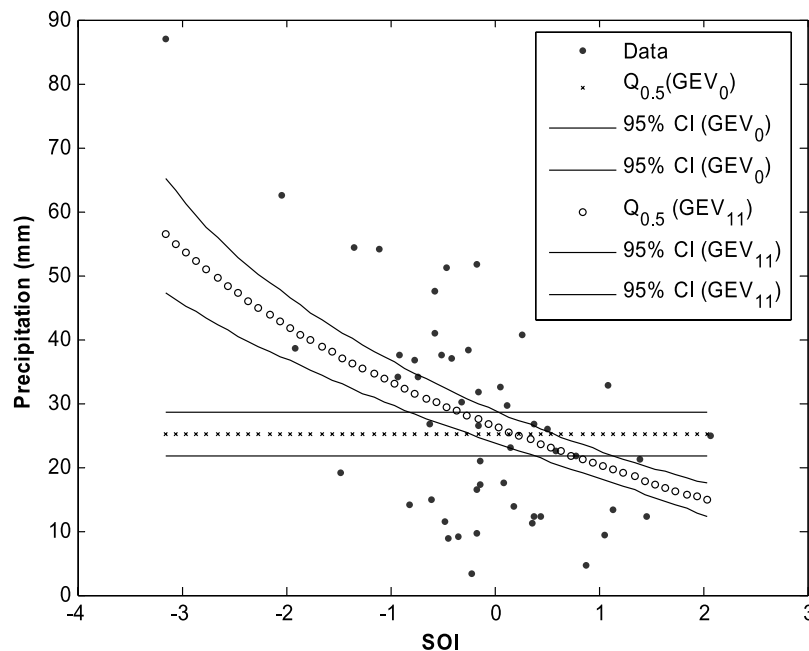


Figure 9. GML estimators of the median and 95% credible intervals conditional upon values of the SOI, obtained by the GEV0 and GEV11 models.

assessment in the case of nonstationarity. Indeed, the use of the common notion of “return period” is no longer appropriate in a nonstationary framework. The return period associated to any extreme event value depends on time. Risk assessment should then be carried out through integrating the risk level throughout the life time of a structure, or by considering the worst case scenario, which may occur toward the end of the life time of the structure.

[57] **Acknowledgments.** The financial support provided by the Climate Change Action Fund (CCAF), the Natural Sciences and Engineering Research Council of Canada (NSERC), the Canada Research Chair Canada, and the OURANOS Consortium is gratefully acknowledged. The authors wish also to thank Renaud Patry for his assistance. The paper has been improved by helpful comments from the Associate Editor and two anonymous reviewers.

References

- Aitkin, M., R. J. Boys, and T. J. Chadwick (2005), Bayesian point null hypothesis testing via the posterior likelihood ratio, *Stat. Comput.*, *15*, 217–230.
- Bayarri, M. J., and J. Berger (2000), P-values for composite null models (with discussion), *J. Am. Stat. Assoc.*, *95*, 1127–1142.
- Clarke, R. T. (2002), Estimating trends in data from the Weibull and a generalized extreme value distribution, *Water Resour. Res.*, *38*(6), 1089, doi:10.1029/2001WR000575.
- Coles, G. S. (2001), *An Introduction to Statistical Modeling of Extreme Values*, 208 pp., Springer, New York.
- Cunderlik, J. M., and T. B. M. J. Ouarda (2006), Regional flood-duration-frequency modeling in the changing environment, *J. Hydrol.*, *318*, 276–291.
- Dose, V., and A. Menzel (2004), Bayesian analysis of climate change impacts in phenology, *Global Change Biol.*, *10*, 259–272, doi:10.1111/j.1529-8817.2003.00731.x.
- El Adlouni, S., A.-C. Favre, and B. Bobée (2006), Comparison of methodologies to assess the convergence of Markov chain Monte Carlo methods, *Comput. Stat. Data Anal.*, *50*(10), 2685–2701.
- Fisher, R. A., and L. H. C. Tippett (1928), Limiting forms of the frequency distribution of the largest or smallest member of a sample, *Proc. Cambridge Philos. Soc.*, *24*, 180–190.
- Gelman, A., J. Carlin, H. Stern, and D. Rubin (1995), *Bayesian Data Analysis*, CRC Press, Boca Raton, Fla.
- Gilks, W., S. Richardson, and D. Spiegelhalter (1996), *Markov Chain Monte Carlo Methods in Practice*, CRC Press, Boca Raton, Fla.
- Hamilton, J. (1991), A quasi-Bayesian approach to estimating parameters for mixtures of normal distributions, *J. Bus. Econ. Stat.*, *9*, 27–39.
- Hastings, W. (1970), Monte Carlo sampling methods using Markov chains and their applications, *Biometrika*, *57*, 97–109.
- Hosking, J. R. M. (1990), L-moments: Analysis and estimation of distributions using linear combinations of order statistics, *J. R. Stat. Soc.*, *52*, 105–124.
- Hosking, J. R. M., J. R. Wallis, and E. F. Wood (1985), Estimation of the generalized extreme-value distribution by the method of probability-weighted moments, *Technometrics*, *27*, 251–261.
- Intergovernmental Panel on Climate Change (2001), *Climate Change 2001: Impacts, Adaptation and Vulnerability*, Cambridge Univ. Press, New York.
- Jain, S., and U. Lall (2001), Floods in a changing climate: Does the past represent the future?, *Water Resour. Res.*, *37*, 3193–3205.
- Jenkinson, A. F. (1955), The frequency distribution of the annual maximum (or minimum) of meteorological elements, *Q. J. R. Meteorol. Soc.*, *81*, 158–171.
- Katz, R. W., M. B. Parlange, and P. Naveau (2002), Statistics of extremes in hydrology, *Adv. Water Resour.*, *25*, 1287–1304.
- Kharin, V. V., and F. W. Zwiers (2005), Estimating extremes in transient climate change simulations, *J. Clim.*, *18*, 1156–1173.
- Leadbetter, M. R., G. Lindgren, and H. Rootzen (1983), *Extremes and Related Properties of Random Sequences and Processes*, 336 pp., Springer, New York.
- Madsen, H., P. F. Rasmussen, and D. Rosbjerg (1997), Comparison of annual maximum series and partial duration series methods for modeling extreme hydrologic events: 1. At-site modeling, *Water Resour. Res.*, *33*, 747–758.
- Martins, E. S., and J. R. Stedinger (2000), Generalized maximum likelihood GEV quantile estimators for hydrologic data, *Water Resour. Res.*, *36*, 737–744.
- Metropolis, N., A. Rosenbluth, M. Rosenbluth, A. Teller, and E. Teller (1953), Equations of state calculations by fast computing machines, *J. Chem. Phys.*, *21*, 1087–1092.
- Morrison, J. E., and J. A. Smith (2002), Stochastic modeling of flood peaks using the generalized extreme value (GEV) distribution, *Water Resour. Res.*, *38*(12), 1305, doi:10.1029/2001WR000502.
- Ouarda, T. B. M. J., J. W. Labadie, and D. G. Fontane (1997), Indexed sequential hydrologic modeling for hydropower capacity estimation, *J. Am. Water Resour. Assoc.*, *33*, 1337–1349.
- Ouarda, T. B. M. J., C. Girard, G. Cavadas, and B. Bobée (2001), Regional flood frequency estimation with canonical correlation analysis, *J. Hydrol.*, *254*, 157–173.

- Reis, D. S., and J. R. Stedinger (2005), Bayesian MCMC flood frequency analysis with historical information, *J. Hydrol.*, 313, 97–116.
- Sankarasubramanian, A., and U. Lall (2003), Flood quantiles in a changing climate: Seasonal forecasts and causal relations, *Water Resour. Res.*, 39(5), 1134, doi:10.1029/2002WR001593.
- Scarf, P. A. (1992), Estimation for a four parameter generalized extreme value distribution, *Commun. Stat. Theory Methods.*, 21, 2185–2201.
- Smith, R. L. (1985), Maximum likelihood estimation in a class of non-regular cases, *Biometrika*, 72, 67–92.
- Smith, R. L. (1989), Extreme value analysis of environmental time series: An application to trend detection in ground-level ozone (with discussion), *Stat. Sci.*, 4, 367–393.
- Stedinger, J. R., R. M. Vogel, and E. Foufoula-Georgiou (1993), Frequency analysis of extreme events, in *Handbook of Hydrology*, edited by D. R. Maidment, pp. 1–66, McGraw-Hill, New York.
- Venkataraman, S. (1997), Value at risk for a mixture of normal distributions: The use of quasi-Bayesian estimation technique, in *Economic Perspectives*, pp. 2–13, Fed. Reserve Bank of Chicago, Chicago, Ill.
- Wang, X. L. and V. Swail (2004), Climate change signal and uncertainty in projections of ocean wave heights, paper presented at 8th International Workshop on Wave Forecast and Hindcast, Environ. Can., Oahu, Hawaii, 14–19 Nov.
- Wang, X. L., F. W. Zwiers, and V. Swail (2004), North Atlantic Ocean wave climate scenarios for the 21st century, *J. Clim.*, 17, 2368–2383.
- Zhang, X., K. D. Harvey, W. D. Hogg, and T. R. Yuzyk (2001), Trends in Canadian streamflow, *Water Resour. Res.*, 37, 987–999.
- Zhang, X., F. W. Zweirs, and G. Li (2004), Monte Carlo experiments on the detection of trends in extreme values, *J. Clim.*, 17, 1945–1952.

B. Bobée, S. El Adlouni, and T. B. M. J. Ouarda, Centre Eau, Terre and Environnement, Institut National de la Recherche Scientifique, University of Quebec, 490, de la Couronne, Quebec, QC, Canada G1K 9A9. (salaheddine_el-adlouni@ete.inrs.ca)

R. Roy, OURANOS Consortium on Climate Change, 550 Sherbrooke Ouest, Tour Ouest, 19eme Etage, Montreal, QC, Canada H3A 1B9.

X. Zhang, Climate Research Branch, Climate Monitoring and Data Interpretation Division, Meteorological Service of Canada, Environment Canada, 4905 Dufferin Street, Downsview, ON, Canada M3H 5T4.